PHYSICAL REVIEW C **71**, 011303 (2005)

Identification of excited states in $^{61}_{31}Ga_{30}$: Mirror nuclei in the upper fp shell

L-L. Andersson, E. K. Johansson, J. Ekman, D. Rudolph, R. du Rietz, and C. Fahlander
Department of Physics, Lund University, S-22100 Lund, Sweden

C. J. Gross, P. A. Hausladen, and D. C. Radford
Physics Division, Oak Ridge National Laboratory, Oak Ridge, Tennessee 37830

G. Hammond
School of Chemistry and Physics, Keele University, Keele, Staffordshire, ST5 5BG, United Kingdom
(Received 6 September 2004; published 24 January 2005)

In the fusion-evaporation reaction $^{40}Ca + ^{24}Mg$ at 104 MeV beam energy, excited states have been observed for the first time in the isotope $^{61}_{31}Ga_{30}$. The experimental setup comprised the Ge array CLARION, a recoil mass spectrometer and, in its focal plane, an ionization chamber. Five transitions in ^{61}Ga are identified, out of which a cascade of three transitions has been established by means of recoil-$\gamma\gamma$ coincidences. The strong transitions at 271 keV in ^{61}Ga and 124 keV in ^{61}Zn are viewed as the "mirror" $5/2^- \rightarrow 3/2^-$ ground-state transitions. The rather large energy difference of 150 keV is suggested to arise from Coulomb monopole contributions. Shell-model calculations support this interpretation.

DOI: 10.1103/PhysRevC.71.011303 PACS number(s): 21.60.Cs, 23.20.En, 23.20.Lv, 27.40.+z

The proton and the neutron can be viewed as two states of the nucleon, characterized by an isospin quantum number [1]. Assuming isospin symmetry, mirror nuclei, i.e., pairs of nuclei where the number of protons and neutrons are interchanged, would reveal identical level schemes. However, the electromagnetic interaction between protons obviously breaks this symmetry, which leads to small differences between level energies of analog states in pairs of mirror nuclei—the so-called mirror energy differences (MED).

During the past decade the experimental knowledge of $T = 1/2$ and $T = 1$ mirror nuclei in the $1f_{7/2}$ shell has increased substantially (see, e.g., Refs. [2–8]). This continuing progress has been accompanied with detailed theoretical studies and refinements, for example, in Refs. [4,6,7,9]. The observed MED values, typically 10–100 keV, are readily explained by Coulomb monopole effects—e.g., slightly different shapes or radii—and Coulomb multipole effects, which are sensitive to the alignment of pairs of protons.

In nuclei close to the center of the $1f_{7/2}$ shell, Coulomb monopole effects arise from significant $2p_{3/2}$ admixtures into the ground state wave functions, which decrease gradually towards terminating states. In nuclei below and above the rather well isolated $1f_{7/2}$ shell, differences in configurations of adjacent states may cause significant changes in Coulomb monopole contributions manifested as sudden changes in observed MED diagrams. One such example is the $\sim$300 keV drop in MED between the $11/2^-$ and $13/2^-$ states in the $A = 35$ and $A = 39$ mirror systems, which can be explained by radial effects as well as a hitherto overlooked electromagnetic spin-orbit contribution [10]. The latter is sensitive to single-particle excitations between orbits of opposite spin-orbit couplings and may hence reoccur in the upper fp shell, i.e., in the $T_z = \pm 1/2$, $A = 57, 59, 61$ mirror pairs. While some basic knowledge of the neutron-deficient nuclei ^{57}Cu [11] and ^{59}Zn [12] exists, only ground-state half-life measurements based on fragmentation reactions [13,14] and recent β-decay studies [15,16] are available for ^{61}Ga.

In the present paper we report on the observation of excited states in ^{61}Ga and compare its excitation scheme to the rather well known mirror nucleus ^{61}Zn [17–19]. Interestingly, Ref. [16] showed that the $3/2^-$ ground state of ^{61}Ga is bound by only 190(50) keV, which can imply particle-decaying excited states as well.

The experiment was conducted at the Holifield Radioactive Ion Beam Facility at Oak Ridge National Laboratory. In fusion-evaporation reactions of a ^{40}Ca beam at 104 MeV, impinging on a 99.92% isotropically enriched ^{24}Mg target foil of thickness 0.3 mg/cm^2, ^{64}Ge compound nuclei are formed. The $^{61}_{31}Ga_{30}$ nuclei are then produced via the evaporation of one proton and two neutrons.

The Ge detector array CLARION [21] was used to detect the γ radiation at the target position. At the time of the experiment CLARION comprised ten clover detectors. These detectors were placed in a three-ring construction at 90°, 132°, and 154° with respect to the beam axis. The rings consisted of five, three, and two clover detectors, respectively. Each clover contains four Ge crystals, each of which is electrically twofold segmented. This construction allows for add-back and high accuracy event-by-event Doppler corrections.

Add-back is used to reconstruct the energy of Compton scattered γ rays. It is performed if (i) two γ rays are detected within the same clover with a time separation of 30 ns or less and (ii) if the individual energy deposited exceeds a chosen add-back threshold of 20 keV. For a γ-ray energy of $\sim$1 MeV these corrections resulted in a 25% increase in statistics.

As the recoiling nuclei are moving at some 4.3% of the speed of light, the γ-ray energies have to be corrected to account for the Doppler shift and broadening. These corrections require a determination of the emission angles of the γ rays with respect to the velocity vectors of the recoiling

nuclei. The latter are well defined for the residues of interest, as the recoils have to lie in a narrow cone around the beam axis to enter the recoil mass spectrometer (see details in the next paragraph). Due to the physical size of the Ge detectors, the angle at which a γ ray is detected usually differs slightly from the nominal angle at which the detector is placed. Using the side channel information of the segmented crystals, more precise emission angles can be derived [20], which results in a more precise determination of the emitted γ-ray energy. Since the velocity of a recoiling nucleus depends on its kinetic energy, which is measured in the ionization chamber (see below), an event-by-event velocity correction can be performed to further improve the energy resolution of the γ rays. The combination of γ-detection angle and recoil velocity corrections leads to a $\sim$30% ($\sim$10%) improvement of the full width at half maximum (FWHM) of the peaks in the γ-ray spectra in a single crystal at 90° (154°).

After the particle evaporation and prompt γ-decay processes, the reaction products are recoiling from the thin target into a recoil mass spectrometer (RMS) before finally being stopped in an ionization chamber (IC). The RMS [21] separates the recoiling nuclei in mass-to-charge ratio A/Q, where Q represents a nominal charge state of the ions. The RMS was run in converging mode and tuned to center recoils of mass $A = 62$ with charge state $Q = 18.1$ and recoil energy $E = 58.2$ MeV. The noninteger value of Q implies that the $A = 62$ recoils reach the focal plane slightly to the right of the center. Since the RMS has an A/Q acceptance greater than $\pm 4\%$ this setting also allowed recoils of mass $A = 61$ to impinge on the left-hand side of the A/Q dispersed focal plane.

The horizontal position (the A/Q value) is determined by a position-sensitive grid placed inside the IC [21]. The recoiling $A = 61$ nuclei are well separated from scattered beam and other recoiling nuclei using a two-dimensional gate in a plot showing the position of the recoils in the IC versus the total energy deposited in the left-hand side of the IC.

The anode of the position-sensitive IC is split into three segments along the beam direction. The IC was filled with isobutane gas at a pressure of 16.5 torr to put the recoils to a complete stop and to let the energy loss in the three parts of the IC be approximately equal. According to the Bethe-Bloch formula, the fractional energy loss in the three parts of the anode in the IC is proportional to the Z value, and inversely proportional to the total kinetic energy of the recoils. The latter dependence can easily be removed by mathematical procedures, which are described in detail in Ref. [22].

In the next step the modified energy-loss signals, or combinations of these, have been correlated with γ rays detected in CLARION. A number of energy-loss spectra have been studied in coincidence with the known, intense, and clean $A = 61$ transitions at 970 keV (^{61}Cu) and 124 keV (^{61}Zn) [17,18]. A comparison of these spectra resulted in an approach using the ratio between the energy loss in the first and the third part, R_{13}, which improved the Z separation with respect to the traditional usage of the sum of the energy losses in the first and the second part of the IC [21,22].

There are three isotopes of mass $A = 61$ produced in the present fusion-evaporation reaction; $^{61}_{29}Cu_{32}$, $^{61}_{30}Zn_{31}$, and $^{61}_{31}Ga_{30}$. Each of these will peak at slightly different values of

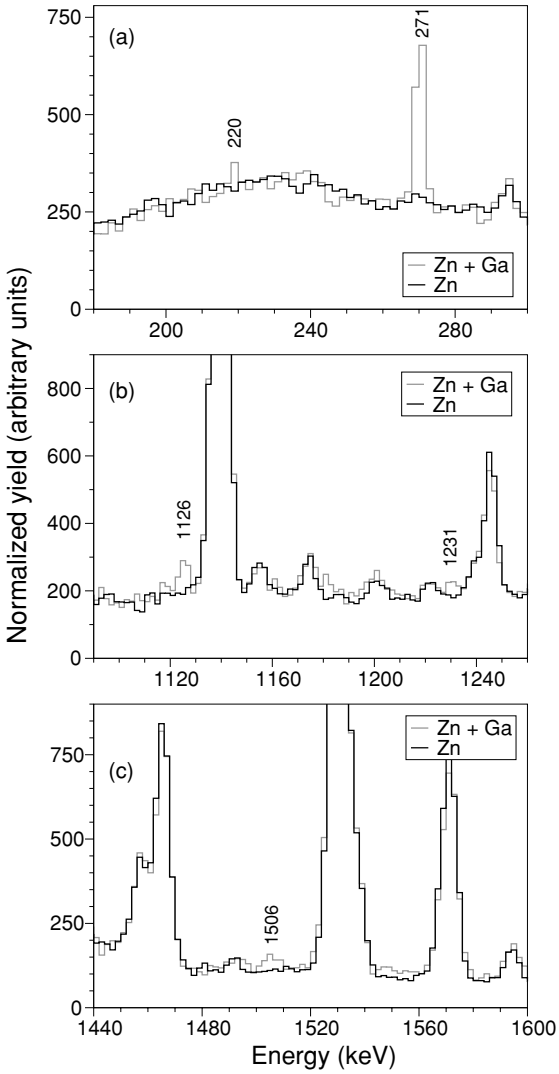

FIG. 1. Normalized γ-ray spectra containing transitions from ^{61}Ga and ^{61}Zn (gray) and only ^{61}Zn (black). The three panels show different energy regions. Energy labels are in keV.

R_{13}. By incrementing γ-ray spectra containing recoils with R_{13} restricted around the known peak positions for ^{61}Cu and ^{61}Zn and performing a careful fractional subtraction, it is possible to obtain clean ^{61}Cu and ^{61}Zn γ-ray spectra. The black γ-ray spectra in Fig. 1(a–c) show parts of the clean ^{61}Zn spectrum. The overlaid gray spectrum in Fig. 1 is correlated with a range of R_{13} values expected for ^{61}Ga. Even for this spectrum, small "contaminations" from ^{61}Cu have been subtracted, and any difference between the gray and the black spectrum will hence indicate the candidates for γ-ray transitions from ^{61}Ga. Figure 1(a) comprises the most prominent candidate at 271 keV. Similarly, four weak transitions can be distinguished at 220, 1126, 1231, and 1506 keV.

Figure 2 proves that the peak at 271 keV indeed belongs to ^{61}Ga. The energy loss ratio R_{13} is shown for the 271 keV line and compared to those of the previously mentioned transitions from ^{61}Cu and ^{61}Zn. It reaches its maximum at a value of R_{13} expected for $Z = 31$, i.e., Ga. Table I provides the energies

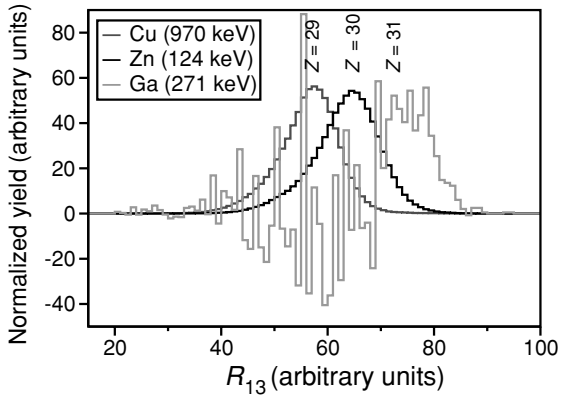

FIG. 2. Normalized spectra of the energy-loss ratio R_{13} from the three $A = 61$ isotopes. The dark gray spectrum is in coincidence with the 970 keV line (^{61}Cu, $Z = 29$); the black spectrum is in coincidence with the 124 keV line (^{61}Zn, $Z = 30$); and the light gray spectrum is in coincidence with the 271 keV line, which is associated with ^{61}Ga ($Z = 31$).

and relative intensities of the transitions belonging to the ^{61}Ga nucleus.

To investigate possible coincidences between the transitions, a recoil gated $\gamma\gamma$ matrix was created. The recoil gate allows only γ rays detected in coincidence with an $A = 61$ recoil in the IC to be included in the matrix, and the recoils must furthermore have a R_{13} value compatible with ^{61}Ga. The matrix will, however, be "contaminated" with ^{61}Zn due to their close placement in the yield versus R_{13} plot (cf. Fig. 2). The 271 keV transition is found to be in coincidence with the transitions at 1126 and 1506 keV. Due to low statistics, no coincidence between the 1126 and the 1506 keV transitions can

TABLE I. Excitation energies, γ-ray energies, relative intensities, and angular distribution ratios for transitions identified in ^{61}Ga and a set of reference transitions in the mirror nucleus ^{61}Zn [17–19].

E_x (keV)	E_γ (keV)	I_γ (%)	R_{154-90}	$I_i^\pi \rightarrow I_f^\pi$
220(1)	220(1)	15(7)		$(1/2^- \rightarrow 3/2^-)$
271(1)	271(1)	100(10)	1.15(16)	$5/2^- \rightarrow 3/2^-$
1397(1)	1126(1)	64(16)		$(9/2^-) \rightarrow 5/2^-$
	1231(1)	22(12)		
2903(2)	1506(1)	39(14)		$(13/2^- \rightarrow 9/2^-)$
88.6(3)	88.6(3)	4(1)[a]	0.84(6)	$1/2^- \rightarrow 3/2^-$
123.7(3)	123.7(3)	150(20)[b]	0.96(4)	$5/2^- \rightarrow 3/2^-$
996.4(4)	872.8(5)	69(2)	0.59(2)	$7/2^- \rightarrow 5/2^-$
	996.4(5)	28(2)	1.49(7)	$7/2^- \rightarrow 3/2^-$
1265(1)	1141(1)	100(3)	1.60(7)	$9/2^- \rightarrow 5/2^-$
2270(1)	1006(1)	13(1)	0.35(2)	$11/2^- \rightarrow 9/2^-$
	1274(1)	34(1)	1.70(8)	$11/2^- \rightarrow 7/2^-$
2399(1)	1403(1)	47(2)	0.85(4)	$9/2^+ \rightarrow 7/2^-$
	2275(2)	2(1)		$9/2^+ \rightarrow 5/2^-$
2796(1)	1532(1)	38(5)	1.66(7)	$13/2^- \rightarrow 9/2^-$
3336(1)	936.9(5)	49(2)	1.70(8)	$13/2^+ \rightarrow 9/2^+$
	1067(1)	8(1)	0.77(6)	$13/2^+ \rightarrow 11/2^-$

[a]Corrected for internal conversion with $\delta(E2/M1) \sim 0.0$.
[b]Corrected for internal conversion with $|\delta(E2/M1)| \sim 1.0$.

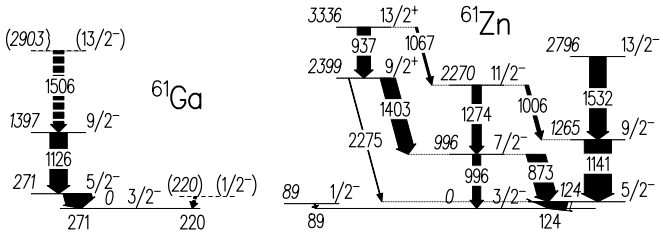

FIG. 3. The proposed level scheme of ^{61}Ga and parts of the known level scheme of the mirror nucleus ^{61}Zn [17–19]. Energy labels are in keV; tentative transitions and levels are dashed; and the widths of the arrows correspond to the relative intensities of the transitions.

be established, but mirror symmetry arguments suggest that the three transitions form the $13/2^- \rightarrow 9/2^- \rightarrow 5/2^- \rightarrow 3/2^-$ cascade in ^{61}Ga. The mirror transitions in ^{61}Zn have energies of 124, 1141, and 1532 keV, respectively [18].

While the 220 keV transition in ^{61}Ga finds a natural counterpart in the 89 keV $1/2^- \rightarrow 3/2^-$ ground-state transition in ^{61}Zn [17], no unique candidate is at hand for the 1231 keV line. The level schemes of the mirror nuclei are shown in Fig. 3.

To add further evidence for the mirror character of the 124 and 271 keV transitions, their multipolarities have been investigated by means of ratios of efficiency-corrected γ-ray yields, Y, measured at two of the three CLARION detector rings. The results are included in Table I. Ratios for known stretched $\Delta I = 2$ reference transitions amount to $R_{154-90} = Y(154^\circ)/Y(90^\circ) \sim 1.6$–$1.7$, while stretched dipole transitions have $R_{154-90} \sim 0.7$–0.8. Both the 271 keV transition in ^{61}Ga and the 124 keV line in ^{61}Zn reveal intermediate values and can thus be considered as mixed $E2/M1\,\Delta I = 1$ transitions.

The relative cross sections of the three $A = 61$ isotopes ^{61}Cu, ^{61}Zn, and ^{61}Ga are estimated from the known or presumed ground-state transitions to 420:110:1.

The experimental MED values of the $A = 61$, $T_z = \pm 1/2$ nuclei, i.e., the difference in excitation energy of analog states in a mirror pair, are illustrated in Fig. 4. The most striking feature is the 150 keV energy difference between the $5/2^- \rightarrow 3/2^-$ ground-state transitions in the two nuclei and, possibly, the 130 keV difference between the presumed $1/2^- \rightarrow 3/2^-$ transitions. In fp shell nuclei such relatively large energy differences have so far only been observed between low-lying single-particle states in the $A = 41$ and $A = 57$ mirror systems [11,23] and between core excited states in the $A = 51$ mirror pair [24].

These differences originate most likely from Coulomb monopole effects such as radial or electromagnetic spin-orbit contributions. The latter has only recently been introduced to explain MED values of up to 350 keV in the mass $A = 35$ and $A = 39$ mirror pairs [10] and should come into play whenever single-nucleon excitations occur between $j = l + 1/2$ orbitals (e.g., $2p_{3/2}$) and $j = l - 1/2$ orbitals (e.g., $1f_{5/2}$ or $2p_{1/2}$). Radial effects can play an important role when nucleon excitations between orbits of different angular momentum occur, since this implies a change in the spatial extent of the charge distribution.

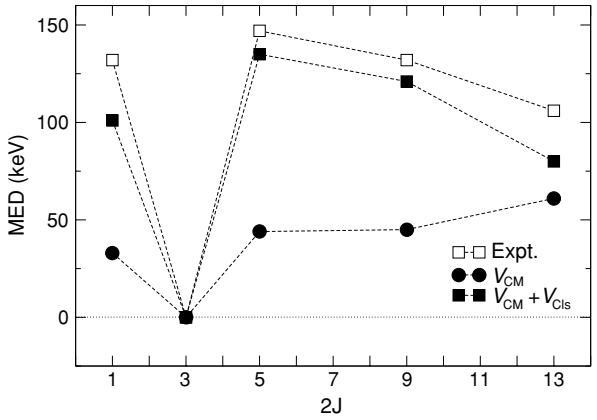

FIG. 4. MED diagram of the $A = 61$ mirror nuclei. Open squares indicate experimental data; filled circles indicate calculated MED values including the V_{CM} component; and filled squares indicate MED values including the $V_{CM} + V_{Cls}$ component. The error bars are smaller than the symbols. See text for details.

Predictions from large-scale shell-model calculations using the shell-model code ANTOINE [25,26] are included in Fig. 4. The calculations were performed in the full fp space containing the $1f_{7/2}$ orbit below and the $2p_{3/2}$, $1f_{5/2}$, and $2p_{1/2}$ orbits above the $N = Z = 28$ shell closures. The configuration space was truncated to allow up to three particle excitations from the $1f_{7/2}$ shell into the upper fp shell. The calculations were performed using the GXPF1 [27,28] with Coulomb interaction, where the two-proton matrix elements are constructed by adding harmonic oscillator Coulomb matrix elements to the bare two-body matrix elements. The interaction used is well adjusted not only for nuclei in the $1f_{7/2}$ shell but also in particular for nuclei at or beyond the $N = Z = 28$ shell closure, i.e., the upper fp shell.

In the first calculation identical single-particle energies for protons and neutrons were used to estimate the Coulomb multipole component, V_{CM}, which takes the effect from the alignment of proton pairs into account. The result is shown as filled circles in Fig. 4. It is seen that the correct sign of the MED values is reproduced, although the predicted MED values are typically 50 to 100 keV smaller than the experimental MED values. These discrepancies may be the result of Coulomb monopole effects, V_{Cm}, which are not yet included in the shell-model calculation.

Since excitations from the $2p_{3/2}$ orbit to the $1f_{5/2}$ and $2p_{1/2}$ orbits are present in the formation of the observed states, the electromagnetic spin-orbit effect, V_{Cls}, comes naturally to mind as a possible explanation. The contribution from the electromagnetic spin-orbit interaction to the single-particle energies can be written as [29]

$$V_{Cls} = (g_s - g_l)\frac{1}{2m_N{}^2c^2}\left\langle \frac{1}{r}\frac{dV_C(r)}{dr}\right\rangle \langle \vec{l}\cdot\vec{s}\rangle, \qquad (1)$$

where $g_s = 5.586$ (-3.828) and $g_l = 1$ (0) are the free gyromagnetic factors for the proton (neutron) and m_N is the nucleon mass. In the present work, V_{Cls} was calculated using harmonic oscillator single-particle wave functions and assuming a charge distribution given by a Fermi distribution with a surface diffuseness parameter and radius equal to 0.5 fm and $1.2 \cdot A^{1/3}$ fm, respectively. The contributions are given in Table II, and the result from a shell-model calculation, where the original single-particle energies have been modified according to Eq. (1), is shown in Fig. 4 as filled squares.

TABLE II. Contribution to the single-particle energies in keV arising from the electromagnetic spin-orbit effect [cf. Eq. (1)].

	$1f_{7/2}$	$2p_{3/2}$	$1f_{5/2}$	$2p_{1/2}$
Protons	−49	−16	66	32
Neutrons	41	13	−55	−26

Obviously, the agreement with the experimental MED values has improved considerably. Other Coulomb monopole contributions such as radial effects—for example, differences in radii between ground states and excited states—appear at first glance to be less important when describing the MED diagram of the $A = 61$ mirror pair. Nevertheless, these effects can be present and large, though they would have to, at least, partially cancel out each other. Naively, one would expect a positive contribution from radial effects for the $5/2^-$ states in both the $A = 57$ and $A = 61$ mirror systems, since these states are formed by exciting a proton (neutron) from a low $l = 1$ $(2p_{3/2})$ orbit to a high $l = 3$ $(1f_{5/2})$ orbit in the $T_z = -1/2(+1/2)$ member. Indeed, the MED value of 260 keV for the $5/2^-$ states in the $A = 57$ mirror nuclei could indicate that such effects are present, because only some 160 keV are accounted for in shell-model calculations including V_{CM} and V_{Cls}, which contribute with ∼25% and ∼75%, respectively. The fact that the $5/2^-$ states in ^{57}Cu and ^{61}Ga are unbound with 333(19) keV and 79(54) keV, respectively, further complicates the situation. One could finally add that in the $A = 59$ mirror pair all Coulomb monopole effects are suppressed because of a high degree of configuration mixing of both proton and neutron excitations in both ^{59}Zn and ^{59}Cu [12]. A full assessment of radial Coulomb monopole contributions to MED diagrams in the upper fp shell thus requires a forthcoming detailed and thorough theoretical investigation.

Last but not least, it is intriguing to take a closer look at the level schemes in Fig. 3. There is no apparent hint of the $9/2^+ \rightarrow 7/2^- \rightarrow 5/2^-$ (1403–873 keV in ^{61}Zn) or the $9/2^+ \rightarrow 7/2^- \rightarrow 3/2^-$ (1403–996 keV in ^{61}Zn) sequence in ^{61}Ga in the present data set, even though the branch through the 2399 keV $9/2^+$ state in ^{61}Zn has about the same intensity as the $13/2^- \rightarrow 9/2^- \rightarrow 5/2^-$ cascade. A possible explanation for the nonobservation of γ-rays decaying from a $9/2^+$ state in ^{61}Ga is a $1g_{9/2}$ proton decay of that level into the ground state of ^{60}Zn. Using $E_x(9/2^+) \sim 2.4$ MeV, together with the known binding energy, one can estimate $Q_p \sim 2.2$ MeV for such a decay, which is very similar to the energetics of $1g_{9/2}$ prompt proton decays from deformed to near spherical states in the mass region [30]. In the present case, however, no significant shape change should be associated with the decay, which further enhances its likelihood.

To summarize, we have observed excited states in ^{61}Ga via recoil-γ coincidences. Three transitions were found to

be in coincidence. Pronounced energy differences in $A = 61$ analog states can to a large extent be explained by a combination of the multipole Coulomb term and the electromagnetic spin-orbit contribution. This interpretation is based on truncated shell-model calculations in the full fp space. The magnitude, sign, and hence significance of other Coulomb monopole terms in explaining the observed MED differences remains to be investigated, preferably through a dedicated theoretical study of mirror nuclei in the upper fp shell.

We would like to thank the staff and the accelerator crew at ORNL for the excellent support during the experiment and F. Nowacki for helpful discussions. This research was supported in part by the Swedish Research Council.

[1] *Isospin in Nuclear Physics*, edited by D. H. Wilkinson (North-Holland, Amsterdam, 1969).
[2] M. A. Bentley *et al*., in *Proceedings Pingst 2000—Selected Topics on N = Z Nuclei*, edited by D. Rudolph and M. Hellström (Bloms i Lund, Sweden, 2000), p. 222.
[3] S. M. Lenzi and P. G. Bizzeti, in *Achievements with the EUROBALL Spectrometer*, edited by W. Korten and S. Lunardi (LNL-IFN(Rep)201, 2004), p. 59.
[4] M. A. Bentley, C. D. O'Leary, A. Poves, G. Martínez-Pinedo, D. E. Appelbe, R. A. Bark, D. M. Cullen, S. Ertürk, and A. Maj, Phys. Lett. **B437**, 243 (1998).
[5] J. Ekman *et al*., Eur. Phys. J. A **9**, 13 (2000).
[6] S. J. Williams *et al*., Phys. Rev. C **68**, 011301(R) (2003).
[7] S. M. Lenzi *et al*., Phys. Rev. Lett. **87**, 122501 (2001).
[8] P. E. Garrett *et al*., Phys. Rev. Lett. **87**, 132502 (2001).
[9] A. P. Zuker, S. M. Lenzi, G. Martínez-Pinedo, and A. Poves, Phys. Rev. Lett. **89**, 142502 (2002).
[10] J. Ekman *et al*., Phys. Rev. Lett. **92**, 132502 (2004).
[11] M. R. Bhat, Nucl. Data Sheets **85**, 415 (1998).
[12] C. Andreoiu *et al*., Eur. Phys. J. A **14**, 317 (2002).
[13] J. A. Winger *et al*., Phys. Rev. C **48**, 3097 (1993).
[14] M. J. López Jiménez *et al*., Phys. Rev. C **66**, 025803 (2002).
[15] M. Oinonen *et al*., Eur. Phys. J. A **5**, 151 (1999).
[16] L. Weissman *et al*., Phys. Rev. C **65**, 044321 (2002).
[17] M. R. Bhat, Nucl. Data Sheets **88**, 417 (1999).
[18] S. M. Vincent *et al*., Phys. Rev. C **60**, 064308 (1999).
[19] O. Izotova *et al*., Phys. Rev. C **69**, 037303 (2004).
[20] E. K. Johansson, Master's thesis, Lund University, LUNFD6/(NFFR-5023)1-47, 2004.
[21] C. J. Gross *et al*., Nucl. Instrum. Meth. Phys. Res. A **450**, 12–29 (2000).
[22] L-L. Andersson, Master's thesis, Lund University, LUNFD6/(NFFR-5022)1-47, 2004.
[23] J. A. Cameron and B. Singh, Nucl. Data Sheets **94**, 429 (2001).
[24] J. Ekman *et al*., Phys. Rev. C **70**, 057305 (2004).
[25] E. Caurier, shell model code ANTOINE, IRES, Strasbourg, 1989-2002.
[26] E. Caurier and F. Nowacki, Acta Phys. Pol. **30**, 705 (1999).
[27] M. Honma, T. Otsuka, B. A. Brown, and T. Mizusaki, Phys. Rev. C **69**, 034335 (2004).
[28] M. Honma, T. Otsuka, B. A. Brown, and T. Mizusaki, Phys. Rev. C **65**, 061301 (2002).
[29] R. J. Blin-Stoyle, in *Isospin in Nuclear Physics*, edited by D. H. Wilkinson (North-Holland, Amsterdam, 1969), Ch. 4.
[30] D. Rudolph *et al*., Phys. Rev. Lett. **80**, 3018 (1998).